Journal of Hydrology 550 (2017) 427–440

Contents lists available at ScienceDirect

Journal of Hydrology

journal homepage: www.elsevier.com/locate/jhydrol

Research papers

Using long-term daily satellite based rainfall data (1983–2015) to analyze spatio-temporal changes in the sahelian rainfall regime

Wenmin Zhang [a,b,*], Martin Brandt [b], Francoise Guichard [c], Qingjiu Tian [a], Rasmus Fensholt [b]

[a] International Institute for Earth System Sciences, Nanjing University, 210023 Nanjing, China
[b] Department of Geosciences and Natural Resource Management, University of Copenhagen, 1350 Copenhagen, Denmark
[c] Centre Nationale de Recherches Météorologiques (CNRM), Meteo-France & UMR CNRS 3589, 42 Avenue Gaspard Coriolis, 31100 Toulouse, France

ARTICLE INFO

Article history:
Received 21 December 2016
Received in revised form 16 May 2017
Accepted 18 May 2017
Available online 19 May 2017
This manuscript was handled by Tim R. McVicar, Editor-in-Chief, with the assistance of Sergio M. Vicente-Serrano, Associate Editor

Keywords:
ARC2
Daily observations
Rain gauge
Rainfall regime
Sahel
Spatio-temporal analysis

ABSTRACT

The sahelian rainfall regime is characterized by a strong spatial as well as intra- and inter-annual variability. The satellite based African Rainfall Climatology Version 2 (ARC2) daily gridded rainfall estimates with a 0.1° × 0.1° spatial resolution provides the possibility for in-depth studies of seasonal changes over a 33-year period (1983–2015). Here we analyze rainfall regime variables that require daily observations: onset, cessation, and length of the wet season; seasonal rainfall amount; number of rainy days; intensity and frequency of rainfall events; number, length, and cumulative duration of dry spells. Rain gauge stations and MSWEP (Multi-Source Weighted-Ensemble Precipitation) data were used to evaluate the agreement of rainfall variables in both space and time, and trends were analyzed. Overall, ARC2 rainfall variables reliably show the spatio-temporal dynamics of seasonal rainfall over 33 years when compared to gauge and MSWEP data. However, a higher frequency of low rainfall events (<10 mm day^{-1}) is found for satellite estimates as compared to gauge data, which also causes disagreements between satellite and gauge based variables due to sensitivity to the number of days with observations (frequency, intensity, and dry spell characteristics). Most rainfall variables (both ARC2 and gauge data) show negative anomalies (except for onset of rainy season) from 1983 until the end of the 1990s, from which anomalies become mostly positive and inter-annual variability is higher. ARC2 data show a strong increase in seasonal rainfall, wet season length (caused by both earlier onset and a late end), number of rainy days, and high rainfall events (>20 mm day^{-1}) for the western/central Sahel over the period of analysis, whereas the opposite trend characterizes the eastern part of the Sahel.

1. Introduction

The Sahel is known as one of the largest semi-arid regions in the world and livelihoods of the sahelian rural population depend primarily on rain-fed agriculture and livestock farming (Leisinger and Schmitt, 1995). The Sahel zone is characterized by high intra-annual variability, affecting water resources and food security (Le Barbé et al., 2002; Nicholson, 1993, 1989; Nicholson and Palao, 1993). The region has experienced several decades of abnormally dry conditions over the past 50 years, including two sequences of extremely dry years in 1972–1974 and 1983–1985 (Hulme, 1992; Le Barbé and Lebel, 1997). These periods, well known as the Sahel droughts, caused severe famines, human and livestock deaths, land abandonment, and large-scale migrations. Sahelian sedentary farmers and pastoralists are consequently forced to adapt to the general decrease in water resources and increase in rainfall variability (Mortimore and Adams, 2001; Romankiewicz et al., 2016). Water availability and timing of precipitation events are key factors for the agricultural crop production (Berg et al., 2009; Sultan et al., 2005) and primary productivity of herbaceous and woody vegetation in the Sahel (Huber et al., 2011). The timing of start of the wet season is pivotal, as most farmers and pastoralists form decisions on cropping and livestock movements on the basis of the occurrence of the first rains (Ingram et al., 2002). Finally, the timing of the seasonal rainfall is decisive; e.g., late season rainfall may lead to high annual/seasonal rainfall sums, however being of little use for crops and herbaceous vegetation, which are both photoperiodic (Breman and Kessler, 2012). Any changes in the overall rainfall regime will have profound impacts on livelihoods. However, the network of rain gauge stations in Africa, and particularly in the Sahel, has decreased significantly in recent years (Eklund et al., 2016; Sanogo et al., 2015), adding considerable uncertainty to datasets based on station data only

* Corresponding author at: Oester Voldgade 10, 1350 Copenhagen, Denmark.
E-mail address: wenminzhg@gmail.com (W. Zhang).

http://dx.doi.org/10.1016/j.jhydrol.2017.05.033
0022-1694/

(e.g., the CRU (Climate Research Unit) rainfall datasets) and analyzes hereof (Eklund et al., 2016), hampering studies of rainfall regime changes. Moreover, the Sahel rainfall spatial heterogeneity is not well captured by the gridded CRU datasets (0.5° spatial resolution) or by widely dispersed station data from gauge observations. Seasonal rainfall is found to vary significantly at scales of a few tens of km (meso-scale) (Nicholson, 2000) and spatial variability at the daily timescales is also high due to the predominantly convective nature of precipitation during the rainy season (Lebel et al., 2003; Laurent et al., 1998a,b).

Precipitation estimates from satellites provide repetitive, timely, objective, and cost-effective information on the spatio-temporal distribution of rainfall. Estimates of with a high spatio-temporal resolution have been available for the African continent since the 1980s from the METEOSAT satellites and provide vital information on rainfall in areas with an insufficient station network (Maidment et al., 2015). A variety of rainfall datasets have been produced using convective cloud top temperature and by applying the cold cloud duration (CCD) technique (Adler et al., 1994). The performance varies considerably, and calibration and evaluations using rain gauges of such CCD based satellite rainfall products are critical (Jobard et al., 2011; Laurent et al., 1998a,b; Love et al., 2004; Nicholson et al., 2003a,b). An acceptable agreement is often found between satellite and gauge data, even though inter-annual variations in bias are commonly found (McCollum et al., 2000; Nicholson et al., 2003a,b). Yet, the satellite data used in these studies mostly covers relatively short periods of time and only decadal or monthly rainfall observations are evaluated (Moron, 1994; Nicholson and Palao, 1993; Sanogo et al., 2015; Maidment et al., 2015). Only two recent studies have analyzed the satellite/gauge relationship on a daily scale over Sahel (Dembélé and Zwart, 2016; Sanogo et al., 2015), both reporting a weak agreement (r^2 below 0.3) between satellite and gauge data.

Advances have been made in understanding the regional circulations and their relationships to water vapour transport in the West African region (Thorncroft et al., 2011). However, most studies of changes in the sahelian rainfall define the rainy season as a fixed set of months (from either gauge or satellite data) (Jobard et al., 2011; Nicholson, 2005; Nicholson et al., 2003a,b; Sealy et al., 2003). The four months from June to September are usually considered as the rainy season since more than 80% of the annual rainfall falls during this period (Lebel et al., 2003; Sanogo et al., 2015). Only a few scholars have studied changes in the Sahel rainfall regime based on variables such as onset and cessation of the rainy season, rainy days, rainfall intensity from gauge/satellite data (Nicholson and Palao, 1993; Sanogo et al., 2015; Dunning et al., 2016) that can only be resolved using daily rainfall data.

In this study we evaluate the use of the satellite based Africa rainfall climatology version 2 (ARC2) dataset (Novella and Thiaw, 2012) (available from 1983 to the present at daily time steps with a 0.1° × 0.1° spatial resolution) in the characterization of the Sahel rainfall regime and changes herein. The high temporal and spatial resolution enables a comprehensive study of spatially distributed rainfall variables describing the rainfall regime (onset and cessation dates, length of the wet season, seasonal rainfall amount, rainy day, intensity and frequency of rainfall events, dry spell characteristics (number, intensity, and cumulative days of dry spells)). All variables are validated against rain gauge data over a 33-year period. The robustness of the ARC2 rainfall metrics and furthermore intercompared with the global coverage MSWEP dataset (Beck et al., 2017) produced also with a daily temporal resolution. The objectives of this study are threefold: (1) to evaluate the agreement between rainfall variables derived from ARC2, MSWEP and available long-term continuous rain gauge data of daily resolution; (2) to analyze selected ARC2 and gauge derived variables over the full time period; (3) to study the spatial variability in temporal trends of ARC2 derived variables.

2. Materials and methods

2.1. Study area

The Sahel extends from the Atlantic Ocean in the west to the Red Sea in the east and constitutes a transition zone between the arid northern and the humid southern eco-regions (Fig. 1). The delineation was derived from the ARC2 average annual rainfall (1983–2015) with northern/southern boundaries of 100 mm and 700 mm, respectively (Lebel et al., 2009). Typically, the rainy season lasts from June to early October with a peak in August (Le Barbé and Lebel, 1997) and is characterized by a high inter-annual variability, with a coefficient of variation of the mean annual rainfall ranging from 15% to 30% (Sivakumar, 1989). The climate is directly linked to the West African Monsoon with a decreasing rate of annual rainfall of approximately 1 mm km^{-1} along a south-north gradient (Lebel et al., 1997; Frappart et al., 2009). The comparison between ARC2 rainfall and gauge measurements focuses on western and central parts of the Sahel, where the availability of gauge measurements without substantial data gaps is more abundant as compared to the eastern Sahel.

2.2. Datasets

2.2.1. ARC2 dataset

The ARC2 (African Rainfall Climatology Version 2) satellite based daily rainfall dataset is available from 1983 – present at a 0.1° × 0.1° spatial resolution (approximately 11 × 11 km). ARC2 builds on ARC1 that is developed using the algorithm applied in the RFE2 (Rainfall Estimation version 2) which is found to be amongst the most reliable products of satellite based datasets covering Africa (Love et al., 2004). The difference as compared to RFE2 is that ARC1 uses only gauge and infra-red data whereas RFE2 uses additional microwave data, which is not available prior to 1995 (Love et al., 2004). Ultimately, ARC2 is a revision of ARC1 with a recalibration of the 1983–2005 period (Novella and Thiaw, 2012).

2.2.2. MSWEP dataset

The global coverage MSWEP (Multi-Source Weighted-Ensemble Precipitation, version 1.2) rainfall dataset is provided with 3-h temporal resolution for the period 1979–2015 in a 0.25° spatial resolution (Beck et al., 2017). MSWEP is developed by merging the highest quality precipitation data sources available as a function of timescale and location from the combined use of rain-gauge measurements, satellite observations, and estimates from atmospheric models (Beck et al., 2017).

2.2.3. Rain gauge dataset

The gauge rainfall is derived from the Global Historical Climatology Network (GHCN-Daily) (Menne et al., 2012). GHCN rainfall measurements from rain gauge stations are considered to be the most accurate and reliable source of precipitation data in the region (Durre et al., 2010). Stations with at least 80% data availability throughout the entire period 1983–2015 were selected as references for the comparison to ARC2 data, leading to the selection of 30 stations distributed from 17°W to 15°E (Fig. 1). No gap-filling of missing daily observations was done. When a record is missing at a given station, the corresponding ARC2 record is discarded to provide the most accurate comparison of datasets.

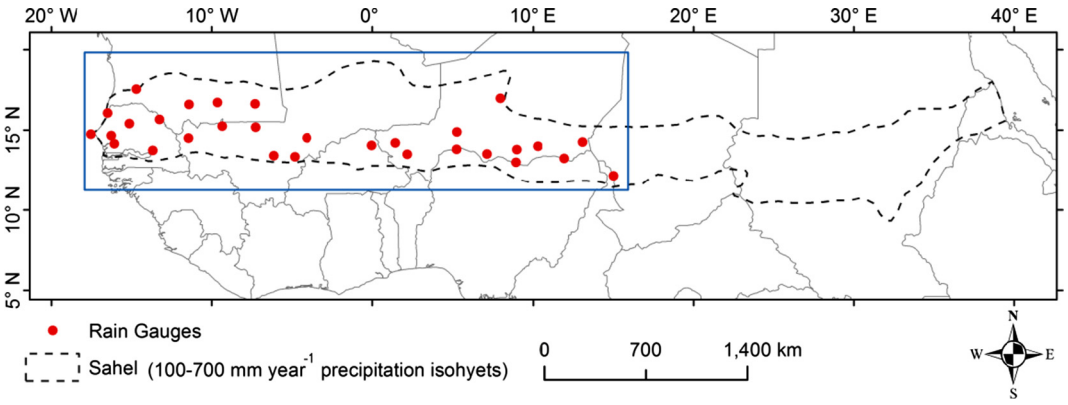

Fig. 1. Study area (Sahel) with 100–700 mm year^{-1} precipitation isohyets (ARC2 mean annual rainfall, 1983–2015) and rain gauges included in this study. Blue rectangle outlines the area used for analysis in Fig. S7. (For interpretation of the references to colour in this figure legend, the reader is referred to the web version of this article.)

2.3. Variables describing the rainfall regime

Variables based on daily rainfall were defined to characterize the rainfall regime (Table 1). Several definitions of onset and end of season exist, based on thresholds of the amount of rainfall recorded during consecutive days (Marteau et al., 2009; Omotosho et al., 2000; Sivakumar, 1988). Fitzpatrick et al. (2015) compared the onset dates calculated from different definitions, datasets, and resolutions and found these choices to have a strong impact on the local patterns of onset dates. To find a criterion that fits both ARC2 and gauge data, we modified the definition proposed by Fitzpatrick et al. (2015) moderately. We defined the onset as the first occurrence of at least 20 mm cumulative rainfall within 7 days after May 1, followed by a total of 20 mm rainfall within the next 20 days (to avoid including so-called "false starts", which do not cause the start of growing season). We determined the end of the rainy season by the occurrence of 20 consecutive days with cumulated rainfall less than 10 mm after September 1. Length of the rainy season was defined as the number of days between the onset and cessation of the rainy season.

The amount of seasonal rainfall was calculated by summing the daily rainfall events ≥1 mm within a rainy season. The number of rainy days was calculated for different levels of intensity: 1–10, 10–20, 20–30, and greater than 30 mm day^{-1}. The intensity of rainfall was calculated by dividing the amount of rainfall within the rainy season by the number of rainy days. To characterize dry spells within a rainy season, three variables were calculated: number of dry spells, length and cumulative dry days (definitions provided in Table 1). Seasonal distribution of the rainfall over the wet season was calculated from the ratio of the rainfall between the first and second half of the season (calculated from the season length and onset).

Table 1
Summary of rainfall variables applied.

Variables	Definitions
Onset of rainy season	The first occurrence of at least 20 mm cumulative rainfall within 7 days after May 1, followed by a total of 20 mm rainfall within the next 20 days
Cessation of rainy season	The occurrence of 20 consecutive days with cumulated rainfall less than 10 mm after September 1
Length of rainy season	Number of days between the onset and the cessation of the rainy season
Seasonal rainfall amount	Rainfall amount during the rainy season.
Rainy day	Number of rainy days (≥1 mm day^{-1}) between the onset and cessation
Frequency	The percent of rainy days: the number of rainy days/ length of rainy season
Intensity	Amount of rainfall within the rainy season amount/the number of rainy days
Seasonal distribution	Ratio of rainfall between the first and second half of the wet season (50% of length of season)
Dry Spell	Rainfall <1 mm day^{-1} during a period of at least seven consecutive days
Number of dry spells	The number of dry spells during rainy season
Length of dry spell	Mean length of dry spells
Cumulative dry days	The total number of dry days accumulated over all dry spells in a rainy season

2.4. Methodology

Both individual 0.1° ARC2 pixels overlaying the rain gauge stations (Fig. 1) and a 3 × 3 pixel window (Fig. S1) were initially tested for the comparison. As the results were nearly identical, only the single pixel overlap method was selected for presentation as this is expected to minimize the bias induced by the scale difference between points and pixels. ARC2 pixels were aggregated to match the MSWEP spatial resolution for the intercomparison of satellite based products.

2.4.1. Standardized rainfall index

Anomalies based on a standardized rainfall index were used to quantify each rainy season in relation to the long-term climatology. Rainfall anomalies are normally computed by averaging the standardized annual variables recorded at each rain gauge station available for a given year (Lamb, 1982; Nicholson, 1985). However, due to the strong spatial variability of the sahelian rainfall and the uneven distribution of the rain gauge network, we applied the index proposed by Ali and Lebel (2009) for any variable V (e.g., seasonal rainfall, onset...):

$$I_v(y) = \frac{V(y) - \bar{V}}{\sigma(V)}$$

where $I_v(y)$ is the V index, $V(y)$ is the regional rainfall variables for year y, $\bar{V}$ and $\sigma(V)$ are the mean and standard deviation, respectively, of V over the region and the reference period 1983–2015. Region refers here to all the rain gauge stations shown in Fig. 1.

2.4.2. Data analysis

To characterize the consistency of rainfall variables between ARC2, MSWEP and gauge data, the linear correlation were performed with Pearson's *t-test*. The correlation analysis was conducted on detrended data (significant linear trends ($p < 0.05$) in rainfall variables were removed) to avoid spurious correlations. Trends were estimated using Sen's slope and assessed with Mann-Kendall test accounting for the effect of serial correlation.

Continuous wavelet analysis was conducted on detrended data to assess changes in rainfall variables as a function of time-scales ranging from inter-annual to decadal variability. Temporal trend analysis was performed to detect changes in trends of rainfall variables including all combinations of sub-periods with a minimum period length of 10 years.

3. Results

3.1. Spatio-temporal correlations between rain gauges and ARC2

Spatio-temporal correlations between rain gauge and ARC2 data were examined by successively analyzing: (i) the rainfall variables across the rain gauge sites; and (ii) the time series of annual standardized seasonal rainfall averaged over the sites.

The comparison of the 33-year seasonal rainfall variables indicates a fair linear relationship between ARC2 and rain gauges for all variables (r values between 0.29 and 0.77) except the dry spell variables with r values between 0.06 and 0.22) (Fig. 2). The onset, cessation, length of the rainy season and the seasonal rainfall amount generally correspond well (Fig. 2a–d). A strong discrepancy is observed in the occurrence of rainfall events lower than 20 mm day^{-1} (1–10 and 10–20 mm day^{-1}) (Fig. 2h), with a pronounced higher number of days of observations in the satellite product as compared to gauge measurements. The higher frequency of satellite rainfall events becomes smaller for events of higher rainfall (20–30 mm day^{-1}) and a lower frequency of the number of strong ARC2 rainfall events (>30 mm day^{-1}) is observed (Fig. 2h). The higher representation of low rainfall from the satellite also results in a higher satellite based number and frequency of rainy days (Fig. 2e–f) and correspondingly lower values of satellite based rainfall intensity (Fig. 2g). While the satellite seasonal rainfall amounts are close to gauge measured rainfall, the observed correspondence includes much more frequent low rainfall events and slightly less frequent strong rainfall events (Fig. S2 Supplementary information). ARC2 versus gauge based seasonal distribution (Fig. 2i) indicates a bias towards more gauge based occurrences of early season rainfall as compared to satellite rainfall. Comparison of satellite and gauge based estimates of dry spell characteristics (Fig. 2j–l) is severely impacted by the higher frequency of satellite based records of low rainfall events, causing much higher gauge based number of dry spells, lengths and cumulative dry days. Similar results are obtained when analyzing 33-year average values of rainfall variables (Fig. S3).

ARC2 derived rainfall variables were compared with corresponding metrics derived from MSWEP (Fig. 3). Overall, a good consistency between ARC2 and MSWEP rainfall metrics was observed for rainfall seasonal timing and seasonal amount (Fig. 3a–d) with r values ranging between 0.69 and 0.86. For the metrics related to the timing/frequency of individual rainfall events (Fig. 3e, f, h) there is a bias towards more observations from MSWEP as compared to ARC2 (especially pronounced for rainfall events of 1–10 mm day^{-1}) causing the calculation of rainfall intensity to be higher for ARC2 as compared to MSWEP (Fig. 3g). The difference in frequency of rainfall events causes the dry spell comparisons to show moderate agreement (r values between 0.23 and 0.27) (Fig. 3j–l).

3.2. Inter-annual variability and trends of rain gauge and ARC2 variables

The temporal consistency of rainfall variables over the 33-year period for both gauge and ARC2 (Fig. 4) was assessed using the correlation coefficients and statistical significance was determined by Pearson's *t-test* accounting for serial correlation (Table 2). The results are generally in line with those obtained for the correlations in Figs. 2 and S3, with the weakest agreement (both ARC2/gauge and ARC2/MSWEP) between data for low rainfall events, intensity, and seasonal distribution. However, the ARC2/gauge correlations of dry spell variables are higher when calculated over time than over space, which suggests that ARC2 better captures inter-annual than spatial fluctuations of dry spells. Clear positive trends are shown in the rainy season length, the seasonal rainfall amount, the number of rainy days, the rain event frequency, and the rainy days above 10 mm day^{-1} (10–20, 20–30 and >30 mm day^{-1}) in both ARC2, MSWEP and gauge data (Table 2). Temporal consistency between ARC2 and MSWEP is found with significant correlations for all rainfall variables during 1983–2015. However, significant trends of MSWEP are only found for cessation, length of rainy season, seasonal rainfall amount, intensity and number of days with rainfall of 10–20 and 20–30 mm day^{-1}, whereas also the onset, number of rainy days, number of days with rainfall of >30 mm day^{-1} and seasonal distribution are characterized by significant trends for ARC2.

Negative anomalies dominated from 1983 to the end of the 1990s, while after this period, more consistent positive anomalies from 2000 to present were observed (Fig. 4c–k). The increase in rainy season length associated with a significantly negative trend in the onset dates of the rainy season is found in both ARC2 and gauge (Fig. 4a and c). Rain gauge data indicates significantly positive trend in the number of rain events from the small (1–10 mm day^{-1}) to the high (>30 mm day^{-1}), which agrees with the results of ARC2, except for the trend of small rainfall events (not significant for ARC2) (Table 2). The ARC2 based rainfall intensity is characterized by a significantly positive trend, which is not supported by the gauge data (Fig. 4g and Table 2). It is noticeable that no significant trends are observed for dry spells in both datasets despite the strong positive trend of seasonal rainfall (Fig. 4m–o and Table 2); i.e., the partial recovery of rainfall observed since the 80s' droughts is not associated with a substantial decrease of dry spells during the monsoon. A significantly negative trend is seen in the seasonal distribution for ARC2 (showing a shift in the ratio between early and late rainfall towards later monsoon rainfall) while no change is observed in gauges (Table 2). Wavelet analysis of rainfall variables from both ARC2 and rain gauges show that inter-annual variability of all rainfall metrics appears to be dominated by shorter year-to-year fluctuations (Figs. 5 and S5). Strong inter-annual fluctuations are observed in in several variables, e.g., the onset and cessation dates (Fig. 5a, b). A higher inter-annual variability in seasonal rainfall amount and the number of rainy days (10–20, 20–30, and >30 mm day^{-1}) is also observed over the past 15 years as compared to the beginning of the time series (Fig. 5d, h–k). Multi-year fluctuations could also be identified for variables of the seasonal timing (Fig. 5a–c).

Trends in ARC2 rainfall variables for various time scale combinations (multi-temporal trend analysis) were determined by Mann–Kendall's tau value (only considering direction) (Fig. 6). Significantly negative trends are dominating for the onset of rainy season and seasonal distribution when end of the time series is around recent years (2007–2015). Significantly positive trends are dominating for length of rainy season, seasonal rainfall amount, intensity and number of rainy days (10–20, 20–30 and >30 mm day^{-1}) for a broad array of temporal combinations mirrored by the predominance of negative trends observed for the trend in onset of rainy season. Almost no significant trends in dry spells are observed regardless of the period of analysis.

3.3. Spatio-temporal trends in ARC2 rainfall variables 1983–2015

Spatio-temporal trends (linear slope based on Sen's slope in corresponding unit year^{-1}, only significant trends at the 90%

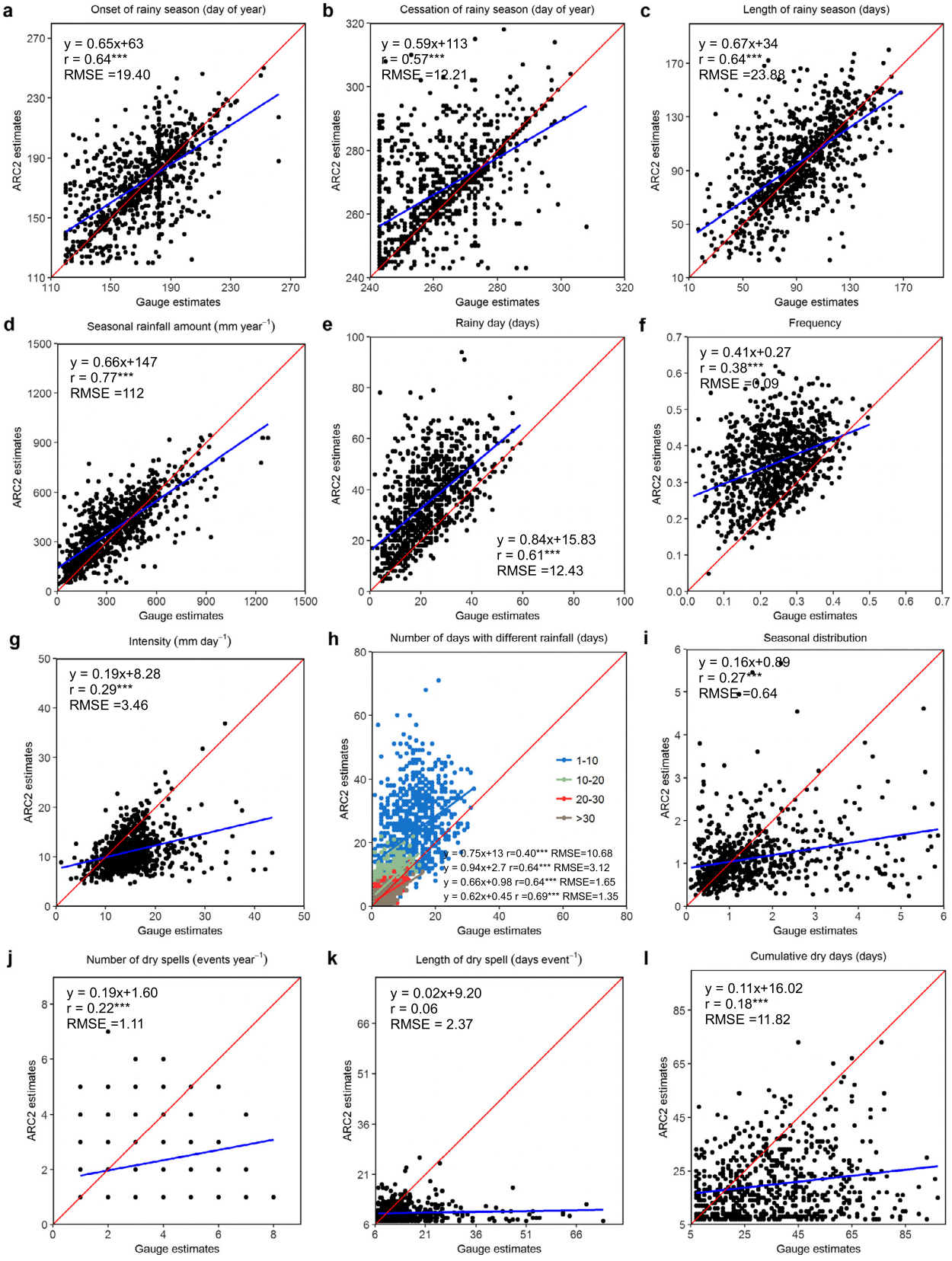

Fig. 2. Scatterplots between annual ARC2 (individual ARC2 pixels overlaying rain gauge stations) and gauge rainfall variables (1983–2015) for all sites (shown in Fig. 1). The blue line is the linear regression line between gauge and ARC2 estimates (except for Fig. 2h, where linear regression lines correspond to the legend point color) and the red line is the 1:1 line. Linear correlation coefficients (r) between ARC2 and gauge rainfall variables are shown and asterisks denote significant correlations ($^{*} = p < 0.1$; $^{**} = p < 0.05$; $^{***} = p < 0.01$). DETAILS: a) onset of rainy season (day of year); b) cessation of rainy season (day of year); c) length of rainy season (days); d) seasonal rainfall amount (mm year^{-1}); e) rainy day (days); f) frequency; g) intensity (mm year^{-1}); h) number of days with rainfall 1–10, 10–20, 20–30, >30 mm day^{-1} (days); i) seasonal distribution; j) number of dry spells (events year^{-1}); k) length of dry spell (days events^{-1}); l) cumulative dry days (days). (For interpretation of the references to colour in this figure legend, the reader is referred to the web version of this article.)

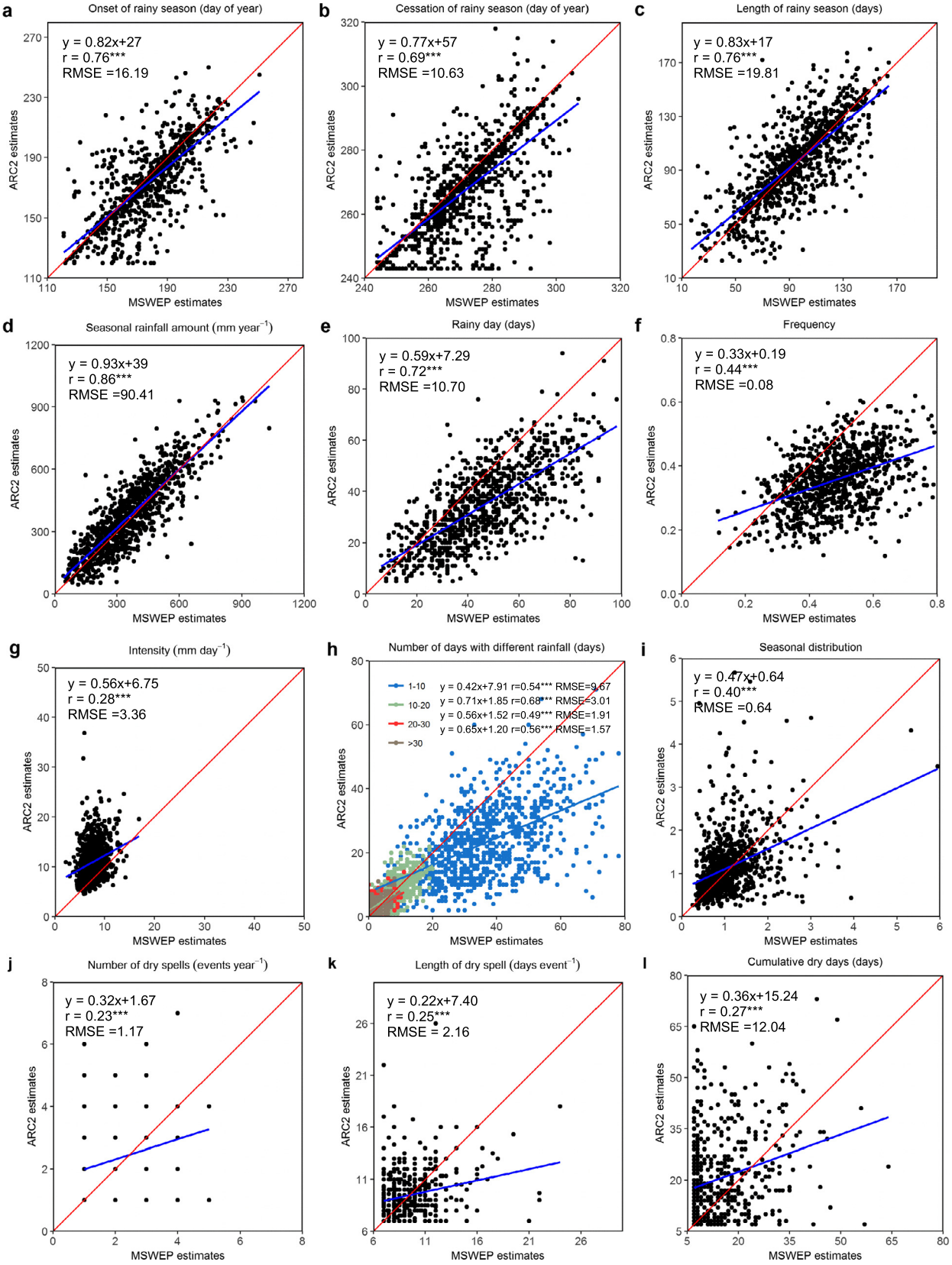

Fig. 3. Scatterplots between annual ARC2 and MSWEP rainfall variables (1983–2015) for all sites (shown in Fig. 1). The blue line is the linear regression line between gauge and ARC2 estimates (except for Fig. 3h, where linear regression lines correspond to the legend point color) and the red line is the 1:1 line. Linear correlation coefficients (r) between ARC2 and gauge rainfall variables are shown and asterisks denote significant correlations ($^{*} = p < 0.1$; $^{**} = p < 0.05$; $^{***} = p < 0.01$). DETAILS: a) onset of rainy season (day of year); b) cessation of rainy season (day of year); c) length of rainy season (days); d) seasonal rainfall amount (mm year^{-1}); e) rainy day (days); f) frequency; g) intensity (mm year^{-1}); h) number of days with rainfall 1–10, 10–20, 20–30, >30 mm day^{-1} (days); i) seasonal distribution; j) number of dry spells (events year^{-1}); k) length of dry spell (days events^{-1}); l) cumulative dry days (days). (For interpretation of the references to colour in this figure legend, the reader is referred to the web version of this article.)

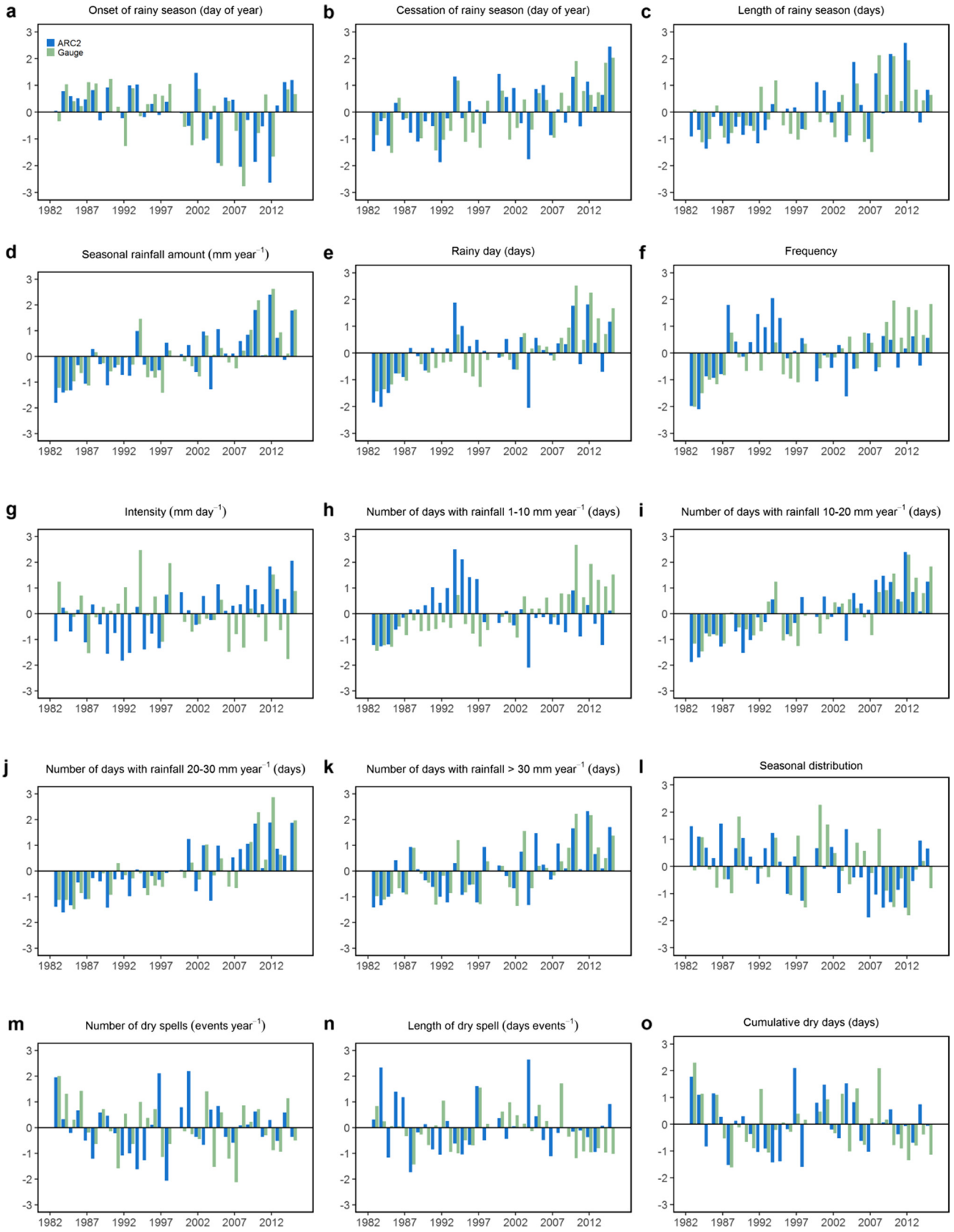

Fig. 4. Inter-annual variability in gauge and ARC2 rainfall variables based on annual rainfall anomalies (from the long-term mean 1983 to 2015). Averages for all gauges and ARC2 pixels overlaying rain gauge stations (Fig. 1). DETAILS: a) onset of rainy season (day of year); b) cessation of rainy season (day of year); c) length of rainy season (days); d) seasonal rainfall amount (mm year^{-1}); e) rainy day (days); f) frequency; g) intensity (mm year^{-1}); h–k) number of days with rainfall 1–10, 10–20, 20–30, >30 mm day^{-1} (days); l) seasonal distribution; m) number of dry spells (events year^{-1}); n) length of dry spell (days events^{-1}); o) cumulative dry days (days).

Table 2
Linear correlation coefficients (r) of annual standardized anomalies between ARC2 and rain gauge rainfall variables (averages for all gauges and ARC2/MSWEP pixels overlaying rain gauge stations) 1983–2015 based on Pearson's significance test accounting for temporal autocorrelation. Trends for ARC2, MSWEP and gauge variables were estimated using the Sen's slope (*slope:* expressing changes in unit per year). Positive (negative) values indicate increasing (decreasing) rainfall variable trends and statistically significant changesare denoted by asterisks (* = $p < 0.1$; ** = $p < 0.05$; *** = $p < 0.01$) with respect to the Mann-Kendall test accounting for temporal autocorrelation.

Variables	*r ARC2-gauge*	*r ARC2-MSWEP*	*trend ARC2*	*trend Gauge*	*trend MSWEP*
Onset of rainy season (day of year)	0.67^{***}	0.81^{***}	-0.17^{*}	-0.20^{**}	−0.006
Cessation of rainy season (day of year)	0.49^{***}	0.80^{***}	0.31^{**}	0.33^{***}	0.23^{**}
Length of rainy season (days)	0.57^{***}	0.82^{***}	0.44^{***}	0.51^{**}	0.17^{**}
Seasonal rainfall amount (mm year^{-1})	0.79^{***}	0.90^{****}	5.48^{***}	5.55^{***}	2.41^{**}
Rainy day (days)	0.51^{**}	0.72^{***}	0.21^{**}	0.39^{***}	0.11
Frequency	0.53^{**}	0.68^{***}	0.0005	0.003^{***}	0.0003
Intensity (mm day^{-1})	0.33^{*}	0.36^{**}	0.07^{***}	−0.04	0.03^{**}
Number of days with rainfall 1–10 mm year^{-1} (days)	0.23	0.43^{**}	−0.02	0.2^{***}	−0.007
Number of days with rainfall 10–20 mm year^{-1} (days)	0.49^{**}	0.79^{***}	0.12^{***}	0.08^{***}	0.09^{***}
Number of days with rainfall 20–30 mm year^{-1} (days)	0.69^{***}	0.62^{***}	0.08^{***}	0.05^{***}	0.03^{*}
Number of days with rainfall >30 mm year^{-1} (days)	0.77^{***}	0.78^{***}	0.04^{***}	0.05^{***}	0.008
Seasonal distribution	0.39^{**}	0.49^{**}	-0.01^{**}	−0.004	−0.0002
Number of dry spells (events year^{-1})	0.16	0.33^{*}	−0.0001	−0.01	−0.007
Length of dry spell (days events^{-1})	0.06	0.42^{**}	0.001	−0.05	−0.004
Cumulative dry days (days)	0.35^{*}	0.38^{**}	−0.03	−0.18	−0.06

confidence level assessed by Mann-Kendall trend test accounting for serial correlation are shown) of ARC2 rainfall variables (Table 1) were calculated for 1983–2015 for the entire Sahel. Rainfall variables of length of the rainy season (Fig. 7c), the seasonal rainfall amount (Fig. 7d), rainy day (Fig. 7e), the frequency of rainy days (Fig. 7f), and the number of days with medium rainfall (10–20 and 20–30 mm day^{-1}) and to some extent, high rainfall (>30 mm day^{-1}) (Fig. 7g and i–k) all show positive trends in most areas of the western/central Sahel. The longer rainy season in the western/central Sahel seems to be associated with an earlier onset date of the rainy season. Much less significant trends are seen in the eastern Sahel and some areas even show significantly negative trends; especially this is the case for medium and high rainfall events, but also the trends in seasonal rainfall and length of the season are negative in some areas of eastern Sahel. The seasonal distribution (Fig. 7l) generally shows a shift in the ratio between early and late rainfall towards later monsoon rainfall from the central part of the Sahel. A scattered pattern of negative trends for dry spell characteristics (number, length of dry spells, and cumulative dry days) are seen primarily in the eastern areas of the Sahel (Fig. 7m–o). Trends calculated from the number of rainy days, frequency, and the number of days with rainfall 1–10 mm day^{-1} (Fig. 7e, f, and h) include localized spurious circular patterns coinciding with the location of rainfall stations. This points towards a data quality issue in the current version of the ARC2 product related to the use of ground observations for the calibration (see Section 4).

4. Discussion

4.1. Reliability of daily ARC2 rainfall estimates: opportunities and uncertainties

We have shown that a general spatio-temporal consistency exists between rainfall variables extracted from ARC2, MSWEP and rainfall station data, which can be used to characterize the rainfall regime in the Sahel. This does not, however, apply to small rainfall events (especially 1–10 mm day^{-1}) (Figs. 2h, S2 and 3h). Estimates in relation to the number of (small) events are substantially biased between ARC2, MSWEP and gauge observations with MSWEP showing the highest number of small events and gauge data the lowest. One plausible explanation could be an inadequacy in the empirically based rainfall algorithm when correcting for the different scale of measurements. Comparing point based measurements with satellite estimates representing larger areas (pixels) inevitably leads to a bias when studying variables with spatial variability (Fensholt et al., 2006). The rainfall of the Sahel is dominated by localized convective cells, which are likely to cause an overrepresentation of small rainfall events from satellite (as it is frequently the case that a small rainfall event will happen somewhere in the ≈121/625 km^2 (ARC2/MSWEP) pixel, but not necessarily at the location of the gauge) and vice versa for large events. The difference in the number of small rainfall events between ARC2/MSWEP and gauge data affects several variables characterizing the rainfall regime (e.g., intensity, dry spell), where a considerable bias exists between daily satellite and gauge data. Therefore, a direct comparison between satellite and gauge rainfall variables influenced by the number of events at the daily time scale seems less appropriate. This may also be partly responsible for the low correlations between ARC2 and daily rain gauge rainfall found by Sanogo et al. (2015) and Dembélé and Zwart (2016). However, even though rainfall variables based on single-day events may be biased due to the difference in scale of measurements, temporal trends in variables from satellite and gauge are still expected to be valid for comparison.

Several satellite rainfall variables characterizing the sahelian rainfall regime were found to correlate well with gauge data and therefore do provide important data for areas with a scarce station network. As very limited rainfall stations provide continuous data in the Sahel (30 stations were found to match the criteria used in this analysis), the ARC2 data provide an opportunity for analyzing changes in the rainfall regime. On the other hand, satellite rainfall estimates are calibrated against gauge data, and the lack of calibration data, particularly in the eastern Sahel, will inevitably increase the uncertainty of the satellite data, even though the climatic mechanism causing rainfall is similar between the west and the east (Sanogo et al., 2015). The consistency between most ARC2 and the global coverage MSWEP variables (except variables derived directly from single-day events) suggest that rainfall regime analysis can be conducted for other dryland areas of the world characterized by convective rainfall systems such as La Plata basin in South America (Nesbitt et al., 2006) or areas of high spatio-temporal variability like inland Australia and parts of the Middle East and India (Nicholson, 2011).

Artifacts around stations derived from the merging portion of the ARC2 algorithm typically occur around the dry season, when there are rain signals in the gauge data and zero rain signals in the satellite information used to define the shape of the rainfall field over space (personal communication with ARC2 producer

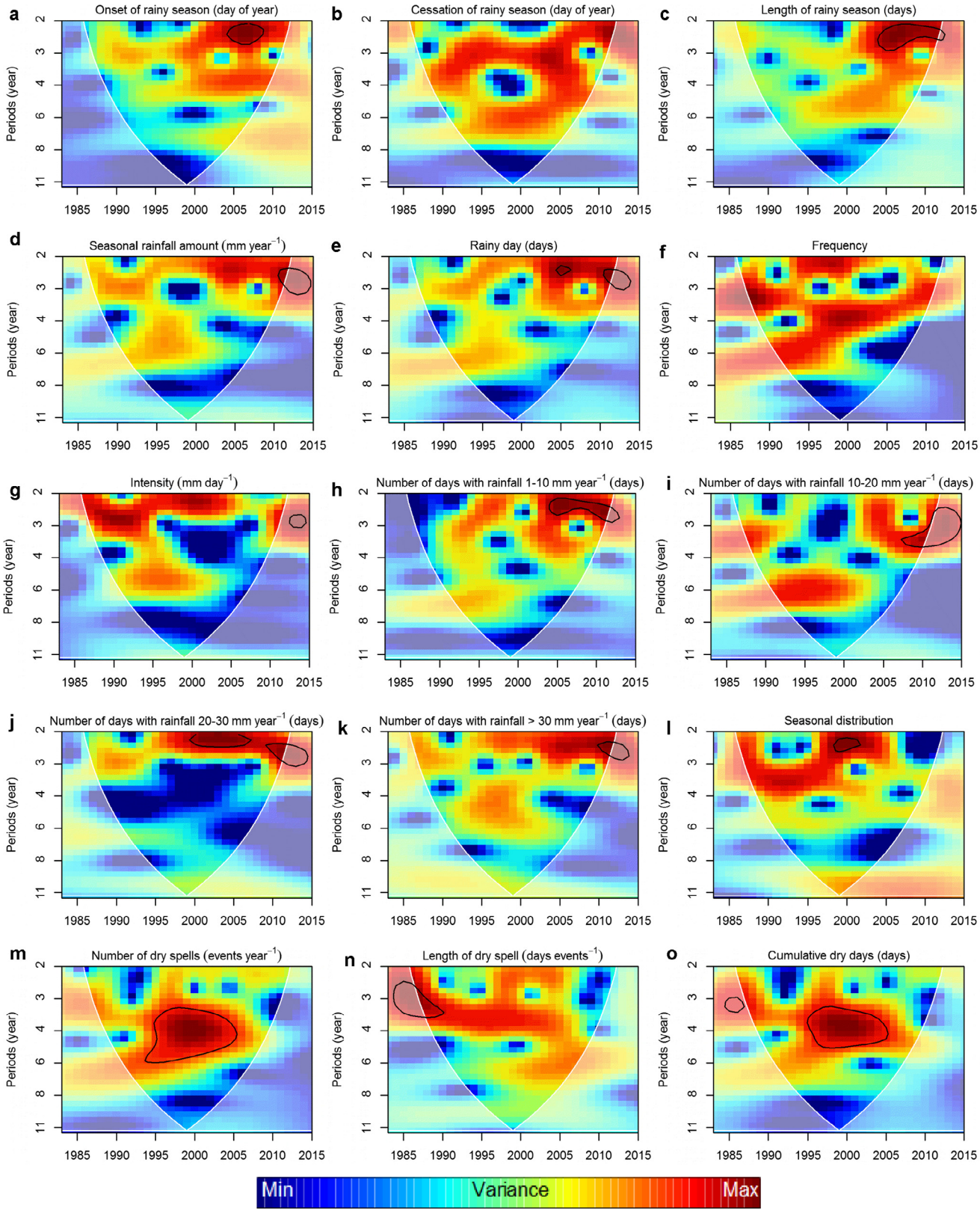

Fig. 5. Continuous wavelet power spectrum of annual rainfall variables based on ARC2 rainfall variables averaged for 30 pixels overlaying gauges. White lines (the so-called cone of influence) delineate the regions under which power can be underestimated due to edge effects. Black contour lines delimit the regions that are statistically significant at the 95% level based on a red noise model [AR(1)] computed for each spectrum as described in Torrence and Compo (1998). DETAILS: a) onset of rainy season (day of year); b) cessation of rainy season (day of year); c) length of rainy season (days); d) seasonal rainfall amount (mm year^{-1}); e) rainy day (days); f) frequency; g) intensity (mm year^{-1}); h, k) number of days with rainfall 1–10, 10–20, 20–30, >30 mm day^{-1} (days); l) seasonal distribution; m) number of dry spells (events year^{-1}); n) length of dry spell (days events^{-1}); o) cumulative dry days (days).

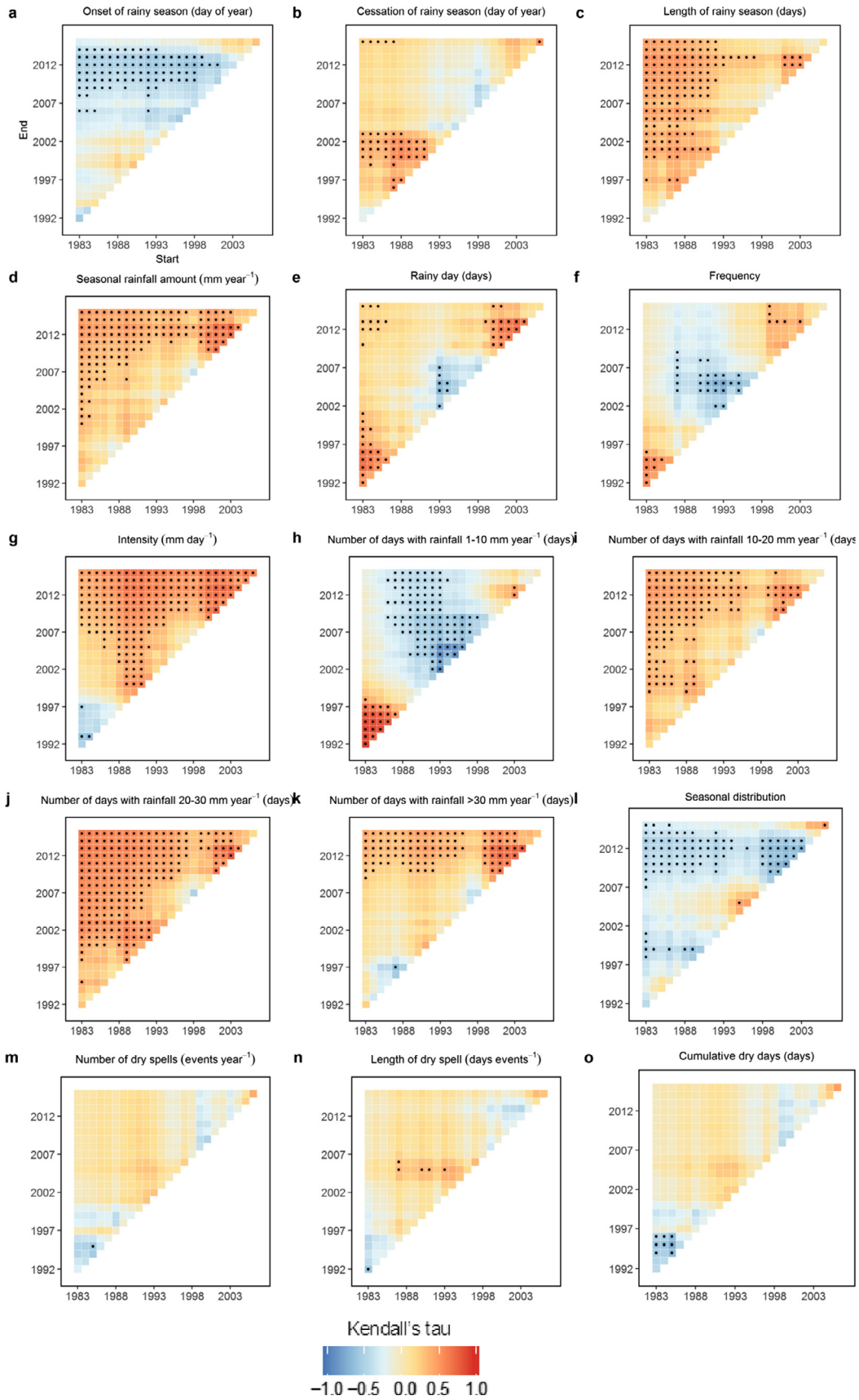

Fig. 6. Trend analysis for ARC2 rainfall variables (average of 30 pixels overlaying gauges) for various periods of at least 10 years in length during 1983–2015. The *x* and *y*-axes indicate the start and ending year, respectively. The scale indicates the magnitude of the trend based on Mann–Kendall's tau coefficient while dots mark a significant trend ($p < 0.05$). DETAILS: a) onset of rainy season (day of year); b) cessation of rainy season (day of year); c) length of rainy season (days); d) seasonal rainfall amount (mm year^{-1}); e) rainy day (days); f) frequency; g) intensity (mm year^{-1}); h–k) number of days with rainfall 1–10, 10–20, 20–30, >30 mm day^{-1} (days); l) seasonal distribution; m) number of dry spells (events year^{-1}); n) length of dry spell (days events^{-1}); o) cumulative dry days (days).

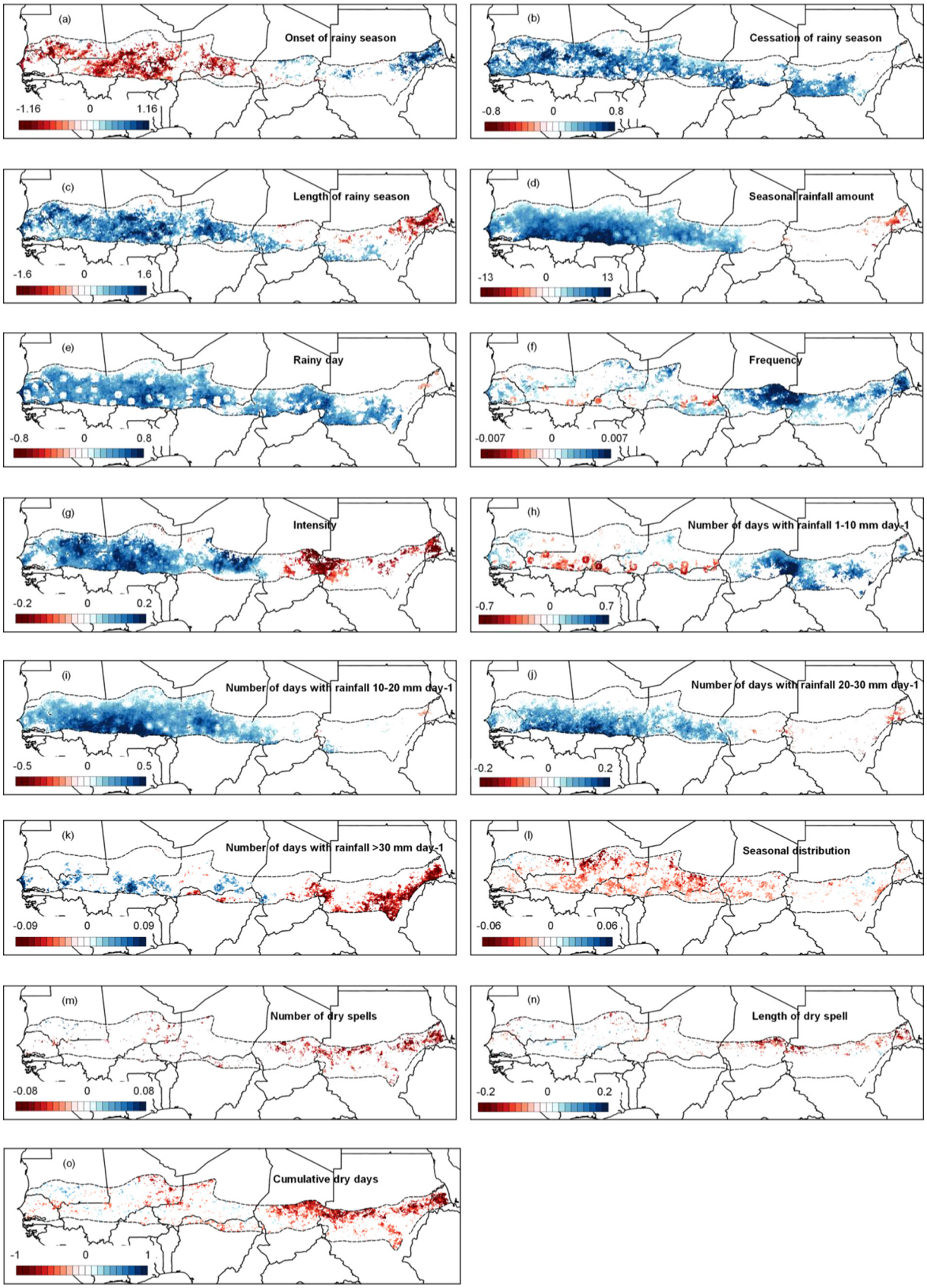

Fig. 7. Trends in ARC2 rainfall variables over Sahel (1983–2015) estimated using the Sen's slope (*slope:* expressing changes in unit per year). Positive (negative) values indicate increasing (decreasing) rainfall variable trends and only statistically significant changes at the 90% confidence level are shown (using Mann-Kendall test accounting for temporal autocorrelation). DETAILS: a) onset of rainy season (day of year); b) cessation of rainy season (day of year); c) length of rainy season (days); d) seasonal rainfall amount (mm year^{-1}); e) rainy day (days); f) frequency; g) intensity (mm year^{-1}); h–k) number of days with rainfall 1–10, 10–20, 20–30, >30 mm day^{-1} (days); l) seasonal distribution; m) number of dry spells (events year^{-1}); n) length of dry spell (days events^{-1}); o) cumulative dry days (days).

Novella, N.). From Fig. 7e, f, and h, it is clear that this issue also extends to the rainy season, which influences rainfall variables being sensitive to the number of small daily rainfall events (e.g., number of rainy days, number of rainy days 1–10 mm day^{-1}, and frequency). Different trends can be observed around rainfall gauge sites as compared to the remaining parts of the region, which yields uncertainty for the reliability of these ARC2 variables. To further investigate the extent of the impact from artifacts on the consistency between ARC2 and rain gauges (Figs. 2 and 4), a comparison was made for gauge rainfall variables averaged over the rain gauges and all pixels of the western/central Sahel region covering rainfall stations (blue rectangle in Fig. 1). Results of correlations between rain gauges and the ARC2 estimates from pixels covering the entire region (Fig. S7) are similar to the results of Figs. 2 and S3, confirming that pixels around rain gauge stations can be used for comparing ARC2 and gauge measurements.

4.2. Implications of rainfall changes 1983–2015

The generally positive trend in ARC2 seasonally summed rainfall for the western and central Sahel during recent decades (Fig. 7d) is well supported by studies based on gauge data at the monthly or annual scale (Frappart et al., 2009; Lebel and Ali, 2009; Maidment et al., 2015; Panthou et al., 2014; Sanogo et al., 2015) and other satellite based rainfall products (Fensholt et al., 2013; Huber et al., 2011; Kaspersen et al., 2011). However, disentangling the seasonal amount of rainfall into different variables characterizing in more details the rainfall regime and changes herein, can provide important information for crops and pasture growth. Our findings show that the increase in annual precipitation is mainly caused by an increase in rainy days with a longer rainy season (an earlier onset) and especially more days with high (extreme) rainfall events (Fig. S6), in line with a gauge based study by Panthou et al. (2014), who also found an increase in inter-annual variability for these variables over the past 15 years. We further observed a shift towards later rainfall at the detriment of early season rainfall. Changes in the seasonal distribution of rainfall affect the sahelian vegetation as late rains are of limited use to crops and herbaceous vegetation, and high rain events can have adverse effects on crop yield and cause increased soil erosion. Moreover, the intra-seasonal distribution of rainfall impacts the herbaceous mass production and species composition in any specific year (Diouf et al., 2016). Several studies have shown that the greening of the Sahel (meaning an increase in net primary productivity monitored by satellites) is strongly linked to rainfall (Dardel et al., 2014) but cannot be explained by rainfall alone (Fensholt and Proud, 2012; Herrmann et al., 2005). These studies usually use annual rainfall sums, however, and new insights into changing vegetation patterns and productivity might be revealed by disentangling seasonal rainfall variables that can be applied at a high spatial resolution and linked with satellite based vegetation productivity data.

At the sub-sahelian scale, we identified areas characterized by an increase in high rainfall events (>30 mm day^{-1}) (e.g. western Senegal, northern Burkina Faso, Southwest Niger). Also, an earlier start of the rainy season, a longer rainy season, and higher seasonal amounts were found in the coastal areas of Senegal, in Mali, and in Niger, but not in the eastern Sahel. The seasonal rainfall amount has been shown to be positively correlated with AMO (Atlantic Multi-decadal Oscillation) over the period 1921–2009 in Diatta and Fink (2014) and several earlier studies, e.g. Hastenrath (1990). Also, a significant increase in summer rainfall related to the warm phases of the AMO was found by Martin and Thorncroft (2014). Recent studies, based on multi-model analysis, also showed that the summer precipitation is projected to increase over the central Sahel, but however to decrease over the western Sahel (2031–2070) as compared to a control period (1960–1999) (Biasutti and Sobel, 2009; James et al., 2015; Monerie et al., 2016). The increase is caused by projected strengthening of the monsoon circulation leading to a northward shift ultimately producing an increase of the rainfall amounts in September–October and a delay in the monsoon withdrawal (Monerie et al., 2016).

5. Conclusion

Spatio-temporal changes in the sahelian rainfall regime, characterized by the onset, cessation, and length of the rainy season; seasonal rainfall amount; number of rainy days; intensity and frequency of rainfall events; and dry spell characteristics, were analyzed from daily observations using both ARC2 and MSWEP satellite estimates and rain gauge data for 1983–2015. Overall, most rainfall variables estimated from ARC2 were found to be consistent with station data and the global coverage MSWEP dataset except for the number of daily observations of small rainfall events (<10 mm day^{-1}). This difference also led to discrepancies in the estimations of rainfall frequency, intensity, and dry spell characteristics. Such discrepancies do not, however, impair the results of the ARC2 per-pixel trend analysis of variables based on the number of daily observations per se. Yet, artifacts were found in the patterns of spatio-temporal trends in ARC2 variables being sensitive to the number of daily rainfall events, particularly for low rainfall events (<10 mm day^{-1}), suggesting that improvements can be made in the implementation of gauge calibration of the current ARC2 product.

Rainfall variables generally showed negative anomalies before the 2000s and positive anomalies in the later period (except onset, seasonal distribution, and dry spell characteristics) for both ARC2 and rain gauge data for the western/central Sahel, supporting the greening of the western/central Sahel over the period 1983–2015. Also, increased inter-annual variability was observed for most variables since year 2000. Linear trend analysis in ARC2 rainfall variables characterizing the rainfall regime showed significantly different patterns between the western/central and eastern Sahel. A strong increase in the seasonal rainfall, wet season length (caused by both earlier onset and late end), number of rainy days, and high rainfall events (>20 mm day^{-1}) was found for the western/central Sahel whereas the opposite trend characterized the eastern part of the Sahel. Analysis of ARC2 daily rainfall estimates is concluded to be valuable for improving the understanding of spatio-temporal trends in the sahelian rainfall regime, albeit with some caution for variables that directly require calculating the number of daily rainfall events. The consistency between trends in ARC2 and MSWEP variables suggest that rainfall regime analyses can be conducted for other dryland areas of the world, where spatio-temporal changes in rainfall are expected to have profound impacts on livelihoods.

Acknowledgements

This study is jointly supported by the European Union's Horizon 2020 research and innovation programme under the Marie Sklodowska-Curie grant agreement (project BICSA number 656564), China Scholarship Council (CSC, 201506190076), and the Danish Council for Independent Research (DFF) project: Greening of drylands: Towards understanding ecosystem functioning changes, drivers and impacts on livelihoods. F Guichard acknowledges support from the NERC/DFID Future Climate for Africa programme under the AMMA-2050 project, grant number NE/M020126/1. The authors thank NOAA/NWS/NCEP/Climate Prediction Center for producing and sharing the Africa Rainfall Climatology Version 2 (ARC2) datasets and Nicholas Novella for personal communication. We also thank NOAA National Climatic Data

Center for sharing the Global Historical Climatology Network (GHCN-DAILY) database. Finally, we thank the anonymous reviewers and editors for their detailed and constructive comments.

Appendix A. Supplementary data

Supplementary data associated with this article can be found, in the online version, at http://dx.doi.org/10.1016/j.jhydrol.2017.05.033.

References

Adler, R., Huffman, G., Keehn, P., 1994. Global tropical rain estimates from microwave-adjusted geosynchronous IR data. Remote Sens. Rev. 11, 125–152. http://dx.doi.org/10.1080/02757259409532262.

Ali, A., Lebel, T., 2009. The Sahelian standardized rainfall index revisited. Int. J. Climatol. 29, 1705–1714. http://dx.doi.org/10.1002/joc.1832.

Beck, H.E., van Dijk, A.I.J.M., Levizzani, V., Schellekens, J., Miralles, D.G., Martens, B., de Roo, A., 2017. MSWEP: 3-hourly 0.25 global gridded precipitation (1979–2015) by merging gauge, satellite, and reanalysis data. Hydrol. Earth Syst. Sci. Discuss. 21, 589–615. http://dx.doi.org/10.5194/hess-21-589-2017.

Berg, A., Quirion, P., Sultan, B., 2009. Weather-index drought insurance in Burkina-Faso: assessment of its potential interest to farmers. Weather Clim. Soc. 1, 71–84. http://dx.doi.org/10.1175/2009WCAS1008.1.

Biasutti, M., Sobel, A.H., 2009. Delayed Sahel rainfall and global seasonal cycle in a warmer climate. Geophys. Res. Lett. 36, 1–5. http://dx.doi.org/10.1029/2009GL041303.

Breman, H., Kessler, J., 2012. Woody Plants in Agro-ecosystems of Semi-arid Regions: With an Emphasis on the Sahelian Countries. Springer Science & Business Media.

Dardel, C., Kergoat, L., Hiernaux, P., Mougin, E., Grippa, M., Tucker, C.J., 2014. Re-greening Sahel: 30 years of remote sensing data and field observations (Mali, Niger). Remote Sens. Environ. 140, 350–364. http://dx.doi.org/10.1016/j.rse.2013.09.011.

Dembélé, M., Zwart, S.J., 2016. Evaluation and comparison of satellite-based rainfall products in Burkina Faso, West Africa. Int. J. Remote Sens. 37, 3995–4014. http://dx.doi.org/10.1080/01431161.2016.1207258.

Diatta, S., Fink, A.H., 2014. Statistical relationship between remote climate indices and West African monsoon variability. Int. J. Climatol. 34, 3348–3367. http://dx.doi.org/10.1002/joc.3912.

Diouf, A.A., Hiernaux, P., Brandt, M., Faye, G., Djaby, B., Diop, M.B., Ndione, J.A., Tychon, B., 2016. Do agrometeorological data improve optical satellite-based estimations of the herbaceous yield in Sahelian semi-arid ecosystems? Remote Sens. 8, 668. http://dx.doi.org/10.3390/rs8080668.

Dunning, C.M., Black, E.C.L., Allan, R.P., 2016. The onset and cessation of seasonal rainfall over Africa. J. Geophys. Res. Atmos. 121, 11405–11424. http://dx.doi.org/10.1002/2016JD025428.

Durre, I., Menne, M.J., Gleason, B.E., Houston, T.G., Vose, R.S., 2010. Comprehensive automated quality assurance of daily surface observations. J. Appl. Meteorol. Climatol. 49, 1615–1633. http://dx.doi.org/10.1175/2010JAMC2375.1.

Eklund, L., Romankiewicz, C., Brandt, M., Doevenspeck, M., Samimi, C., 2016. Data and methods in the environment-migration nexus: a scale perspective. J. Geogr. Soc. Berlin 147, 139–152. http://dx.doi.org/10.12854/erde-147-10.

Fensholt, R., Proud, S.R., 2012. Evaluation of earth observation based global long term vegetation trends – comparing GIMMS and MODIS global NDVI time series. Remote Sens. Environ. 119, 131–147. http://dx.doi.org/10.1016/j.rse.2011.12.015.

Fensholt, R., Rasmussen, K., Kaspersen, P., Huber, S., Horion, S., Swinnen, E., 2013. Assessing land degradation/recovery in the African Sahel from long-term earth observation based primary productivity and precipitation relationships. Remote Sens. 5, 664–686. http://dx.doi.org/10.3390/rs5020664.

Fensholt, R., Sandholt, I., Rasmussen, M.S., Stisen, S., Diouf, A., 2006. Evaluation of satellite based primary production modelling in the semi-arid Sahel. Remote Sens. Environ. 105, 173–188. http://dx.doi.org/10.1016/j.rse.2006.06.011.

Fitzpatrick, R.G.J., Bain, C.L., Knippertz, P., Marsham, J.H., Parker, D.J., 2015. The West African monsoon onset: a concise comparison of definitions. J. Clim. 28, 8673–8694. http://dx.doi.org/10.1175/JCLI-D-15-0265.1.

Frappart, F., Hiernaux, P., Guichard, F., Mougin, E., Kergoat, L., Arjounin, M., Lavenu, F., Koité, M., Paturel, J.-E., Lebel, T., 2009. Rainfall regime across the Sahel band in the Gourma region, Mali. J. Hydrol. 375, 128–142. http://dx.doi.org/10.1016/j.jhydrol.2009.03.007.

Hastenrath, S., 1990. Decadal-scale changes of the circulation in the tropical atlantic sector associated with Sahel drought. Int. J. Climatol. 10, 459–472. http://dx.doi.org/10.1002/joc.3370100504.

Herrmann, S.M., Anyamba, A., Tucker, C.J., 2005. Recent trends in vegetation dynamics in the African Sahel and their relationship to climate. Global Environ. Change 15, 394–404. http://dx.doi.org/10.1016/j.gloenvcha.2005.08.004.

Huber, S., Fensholt, R., Rasmussen, K., 2011. Water availability as the driver of vegetation dynamics in the African Sahel from 1982 to 2007. Global Planet. Change 76, 186–195. http://dx.doi.org/10.1016/j.gloplacha.2011.01.006.

Hulme, M., 1992. Rainfall changes in Africa: 1931–1960 to 1961–1990. Int. J. Climatol. 12, 685–699. http://dx.doi.org/10.1002/joc.3370120703.

Ingram, K.T., Roncoli, M.C., Kirshen, P.H., 2002. Opportunities and constraints for farmers of west Africa to use seasonal precipitation forecasts with Burkina Faso as a case study. Agric. Syst. 74, 331–349. http://dx.doi.org/10.1016/S0308-521X(02)00044-6.

James, R., Washington, R., Jones, R., 2015. Process-based assessment of an ensemble of climate projections for West Africa. J. Geophys. Res. 120, 1221–1238. http://dx.doi.org/10.1002/2014JD022513.Received.

Jobard, I., Chopin, F., Bergès, J.C., Roca, R., 2011. An intercomparison of 10-day satellite precipitation products during West African monsoon. Int. J. Remote Sens. 32, 2353–2376. http://dx.doi.org/10.1080/01431161003698286.

Kaspersen, P.S., Fensholt, R., Huber, S., 2011. A spatiotemporal analysis of climatic drivers for observed changes in Sahelian vegetation productivity (1982–2007). Int. J. Geophys. 2011, 1–14. http://dx.doi.org/10.1155/2011/715321.

Lamb, P.J., 1982. Persistence of Subsaharan drought. Nat. Clim. Change 299, 46–48. http://dx.doi.org/10.1038/299046a0.

Laurent, H., D'Amato, N., Lebel, T., 1998a. How important is the contribution of the mesoscale convective complexes to the Sahelian rainfall? Phys. Chem. Earth 23, 629–633. http://dx.doi.org/10.1016/S0079-1946(98)00099-8.

Laurent, H., Jobard, I., Toma, A., 1998b. Validation of satellite and ground-based estimates of precipitation over the Sahel. Atmos. Res. 47–48, 651–670. doi.org/10.1016/S0169-8095(98)00051-9.

Le Barbé, L., Lebel, T., 1997. Rainfall climatology of the HAPEX-Sahel region during the years 1950–1990. J. Hydrol. 188, 43–73. http://dx.doi.org/10.1016/S0022-1694(96)03154-X.

Le Barbé, L., Lebel, T., Tapsoba, D., 2002. Rainfall variability in West Africa during the years 1950–90. J. Clim. 15, 187–202. http://dx.doi.org/10.1175/1520-0442(2002) 0150187:RVIWAD2.0.CO;2.

Lebel, T., Ali, A., 2009. Recent trends in the Central and Western Sahel rainfall regime (1990–2007). J. Hydrol. 375, 52–64. http://dx.doi.org/10.1016/j.jhydrol.2008.11.030.

Lebel, T., Cappelaere, B., Galle, S., Hanan, N., Kergoat, L., Levis, S., Vieux, B., Descroix, L., Gosset, M., Mougin, E., Peugeot, C., Seguis, L., 2009. AMMA-CATCH studies in the Sahelian region of West-Africa: an overview. J. Hydrol. 375, 3–13. http://dx.doi.org/10.1016/j.jhydrol.2009.03.020.

Lebel, T., Diedhiou, A., Laurent, H., 2003. Seasonal cycle and interannual variability of the Sahelian rainfall at hydrological scales. J. Geophys. Res. Atmos. 108, 1401–1411. http://dx.doi.org/10.1029/2001JD001580 (and 8389).

Lebel, T., Taupin, J.D., D'Amato, N., 1997. Rainfall monitoring during HAPEX-Sahel. 1. General rainfall conditions and climatology. J. Hydrol. 188–189, 74–96. http://dx.doi.org/10.1016/S0022-1694(96)03155-1.

Leisinger, K.M., Schmitt, K., 1995. Survival in the Sahel: an ecological and developmental challenge. International Service for National Agricultural Research.

Love, T.B., Kumar, V., Xie, P., Thiaw, W., 2004. A 20-year daily Africa precipitation climatology using satellite and gauge data. In: Proceedings of the 84th AMS Annual Meeting, Vol. Conference on Applied Climatology, Seattle, WA–(CD-ROM).

Maidment, R.I., Allan, R.P., Black, E., 2015. Recent observed and simulated changes in precipitation over Africa. Geophys. Res. Lett. 42, 8155–8164. http://dx.doi.org/10.1002/2015GL065765.

Marteau, R., Moron, V., Philippon, N., 2009. Spatial coherence of monsoon onset over Western and Central Sahel (1950–2000). J. Clim. 22, 1313–1324. http://dx.doi.org/10.1175/2008JCLI2383.1.

Martin, E.R., Thorncroft, C.D., 2014. The impact of the AMO on the West African monsoon annual cycle. Q. J. R. Meteorol. Soc. 140, 31–46. http://dx.doi.org/10.1002/qj.2107.

McCollum, J.R., Gruber, A., Ba, M.B., 2000. Discrepancy between gauges and satellite estimates of rainfall in Equatorial Africa. J. Appl. Meteorol. 39, 666–679. http://dx.doi.org/10.1175/1520-0450-39.5.666.

Menne, M.J., Durre, I., Vose, R.S., Gleason, B.E., Houston, T.G., 2012. An overview of the global historical climatology network-daily database. J. Atmos. Ocean. Technol. 29, 897–910. http://dx.doi.org/10.1175/JTECH-D-11-00103.1.

Monerie, P.A., Biasutti, M., Roucou, P., 2016. On the projected increase of Sahel rainfall during the late rainy season. Int. J. Climatol. 4383, 4373–4383. http://dx.doi.org/10.1002/joc.4638.

Moron, V., 1994. Guinean and Sahelian rainfall anomaly indices at annual and monthly scales (1933–1990). Int. J. Climatol. 14, 325–341. http://dx.doi.org/10.1002/joc.3370140306.

Mortimore, M.J., Adams, W.M., 2001. Farmer adaptation, change and "crisis" in the Sahel. Global Environ. Change 11, 49–57. http://dx.doi.org/10.1016/S0959-3780(00)00044-3.

Nesbitt, S.W., Cifelli, R., Rutledge, S., a, 2006. Storm morphology and rainfall characteristics of TRMM precipitation features. Mon. Weather Rev. 134, 2702–2721. http://dx.doi.org/10.1175/MWR3200.1.

Nicholson, S.E., 2011. Dryland Climatology. Cambridge University Press. http://dx.doi.org/10.1029/2012EO390010.

Nicholson, S.E., 2005. On the question of the "recovery" of the rains in the West African Sahel. J. Arid Environ. 63, 615–641. http://dx.doi.org/10.1016/j.jaridenv.2005.03.004.

Nicholson, S.E., 2000. The nature of rainfall variability over Africa on time scales of decades to millenia. Global Planet. Change 26, 137–158. doi.org/10.1016/S0921-8181(00)00040-0.

Nicholson, S.E., 1993. An overview of African rainfall fluctuations of the last decade. J. Clim. 6, 1463–1466. http://dx.doi.org/10.1175/1520-0442(1993) 0061463:AOOARF2.0.CO;2.

Nicholson, S.E., 1989. Long-term changes in African rainfall. Weather 44, 46–56. http://dx.doi.org/10.1002/j.1477-8696.1989.tb06977.x.

Nicholson, S.E., 1985. Sub-Saharan rainfall 1981–84. J. Clim. Appl. Meteorol. 24, 1388–1391. http://dx.doi.org/10.1175/1520-0450(1985) 0241388:SSR2.0.CO;2.

Nicholson, S.E., Palao, I.M., 1993. A re-evaluation of rainfall variability in the Sahel. Part I. Characteristics of rainfall fluctuations. Int. J. Climatol. 13, 371–389. http://dx.doi.org/10.1002/joc.3370130403.

Nicholson, S.E., Some, B., McCollum, J., Nelkin, E., Klotter, D., Berte, Y., Diallo, B.M., Gaye, I., Kpabeba, G., Ndiaye, O., 2003a. Validation of TRMM and other rainfall estimates with a high-density gauge dataset for West Africa. Part I: validation of GPCC rainfall product and pre-TRMM satellite and blended products. J. Appl. Meteorol. 42, 1337–1354. http://dx.doi.org/10.1175/1520-0450(2003) 0421355:VOTAOR2.0.CO;2.

Nicholson, S.E., Some, B., McCollum, J., Nelkin, E., Klotter, D., Berte, Y., Diallo, B.M., Gaye, I., Kpabeba, G., Ndiaye, O., 2003b. Validation of TRMM and other rainfall estimates with a high-density gauge dataset for West Africa. Part II: validation of TRMM rainfall products. J. Appl. Meteorol. 42, 1355–1368. http://dx.doi.org/10.1175/1520-0450(2003) 0421355:VOTAOR2.0.CO;2.

Novella, N., Thiaw, W., 2012. Africa Rainfall Climatology Version 2. Washingt. Natl. Ocean. Atmos. Adm..

Omotosho, J.B., Balogun, A.A., Ogunjobi, K., 2000. Predicting monthly and seasonal rainfall, onset and cessation of the rainy season in West Africa using only surface data. Int. J. Climatol. 20, 865–880. http://dx.doi.org/10.1002/1097-0088(20000630)20:8865::AID-JOC5053.0.CO;2-R.

Panthou, G., Vischel, T., Lebel, T., 2014. Recent trends in the regime of extreme rainfall in the Central Sahel. Int. J. Climatol. 34, 3998–4006. http://dx.doi.org/10.1002/joc.3984.

Romankiewicz, C., Doevenspeck, M., Brandt, M., Samimi, C., 2016. Adaptation as by-product: migration and environmental change in Nguith, Senegal. J. Geogr. Soc. Berlin 147, 95–108. http://dx.doi.org/10.12854/erde-147-7.

Sanogo, S., Fink, A.H., Omotosho, J.A., Ba, A., Redl, R., Ermert, V., 2015. Spatio-temporal characteristics of the recent rainfall recovery in West Africa. Int. J. Climatol. 35, 4589–4605. http://dx.doi.org/10.1002/joc.4309.

Sealy, A., Jenkins, G.S., Walford, S.C., 2003. Seasonal/regional comparisons of rain rates and rain characteristics in West Africa using TRMM observations. J. Geophys. Res. Atmos. 108, 4306. http://dx.doi.org/10.1029/2002JD002667.

Sivakumar, M.V.K., 1989. Agroclimatic aspects of rainfed agriculture in the Sudano-Sahelian zone. In: Soil, Crop. water Manag. Sudano-Sahelian Zo. Proc. an Int. Work, pp. 17–38.

Sivakumar, M.V.K., 1988. Predicting rainy season potential from the onset of rains in Southern Sahelian and Sudanian climatic zones of West Africa. Agric. For. Meteorol. 42, 295–305. http://dx.doi.org/10.1016/0168-1923(88)90039-1.

Sultan, B., Baron, C., Dingkuhn, M., Sarr, B., 2005. Agricultural impacts of large-scale variability of the West African monsoon. Agric. For. Meteorol. 128, 93–110. http://dx.doi.org/10.1016/j.agrformet.2004.08.005.

Thorncroft, C.D., Nguyen, H., Zhang, C., Peyrille, P., 2011. Annual cycle of the West African monsoon: regional circulations and associated water vapour transport. Q. J. R. Meteorol. Soc. 137, 129–147. http://dx.doi.org/10.1002/qj.728.

Torrence, C., Compo, G.P., 1998. A practical guide to wavelet analysis. Bull. Am. Meteorol. Soc. 79, 61–78. http://dx.doi.org/10.1175/1520-0477(1998) 0790061:APGTWA2.0.CO;2.